

## Polarity and Conformational Characteristics of Semialiphatic Poly(imide–ester)s

Enrique Saiz,<sup>†</sup> José G. de la Campa,<sup>‡</sup> Javier de Abajo,<sup>‡</sup> and Evaristo Riande<sup>\*,‡</sup>

Departamento de Química Física, Universidad de Alcalá, 28871 Alcalá de Henares, Spain, and Instituto de Ciencia y Tecnología de Polimeros (CSIC), 28006 Madrid, Spain

Received June 9, 1997; Revised Manuscript Received December 15, 1997

**ABSTRACT:** The mean-square dipole moment per repeating unit,  $\langle \mu^2 \rangle/x$ , of the semialiphatic poly(imide–ester) prepared by condensation of *N*-(4-carboxyphenyl)trimellitimide acid and diethylene glycol (PIEDEC) was measured at several temperatures in a dioxane solution. The value of  $\langle \mu^2 \rangle/x$  was 12.70 D<sup>2</sup> at 30 °C, and the temperature coefficient expressed in terms of  $d(\ln \langle \mu^2 \rangle)/dT$  was lower than  $1 \times 10^{-4}$  K<sup>-1</sup>. For comparative purposes, the mean-square dipole moment of *N*-[4-[(decyloxy)carbonyl]phenyl]-4-[(decyloxy)carbonyl]phthalimide (NDDPT), a model compound of the acid residue, was also measured in dioxane solutions and found to be 11.63 D<sup>2</sup> at 30 °C. MD simulations, employing the Amber force field, were used to study the conformational characteristics of NDDPT. These results, in combination with the conformational energies of the flexible residue, permitted a preliminary characterization of the statistics of the chains. Owing to the asymmetry of the acid residue, PIEDEC is a random copolymer of A and B units. The influence of both the distribution of these units and the number of repeating units on the polarity of the poly(ester–imide) is discussed. In general, reasonable agreement between theory and experiment is found. The lack of a strong correlation between the  $\theta$  angles formed by successive rods in the melt may be responsible for the fact that the poly(imide–ester) used in this study does not develop mesomorphic order.

### Introduction

Though the mesogenic character of *N*-(4-carboxyphenyl)trimellitimide makes this compound suitable for the preparation of thermotropic polyesters, mobile mesophases derived from this diacid have been reported only in combination with diphenols.<sup>1–4</sup> In this latter case enantiotropic nematic polyesters have been obtained. However, all attempts to synthesize enantiotropic mobile mesophases failed whenever aliphatic glycols were used in the synthesis of polyesters. Semialiphatic poly(ester–imide)s adopt three different structures in the solid state, namely, a smectic glass and two crystal modifications. Moreover, spacers containing thioether groups yield two different smectic crystal modifications but no enantiotropic liquid crystallization. Poly(ethylene glycol) spacers suppress crystallization and prevent the formation of layer structures.<sup>5,6</sup>

In general, poly(ester–imide)s derived from *N*-(4-carboxyphenyl)trimellitimide are not homopolymers but rather copolymers due to the asymmetry of the diacid residue. The random distribution of head-to-head, head-to-tail, and tail-to-tail units along the chains presumably hinders the development of mesomorphic order. The poly(ester–imide)s obtained by condensation of *N*-(4-carboxyphenyl)trimellitimide acid and poly(ethylene glycol) are readily soluble in common organic solvents and, consequently, offer the possibility of studying their conformational characteristics. Because dipole moments can be measured for chains of any length,<sup>7</sup> this technique is an important tool for the critical interpretation of the polarity of these chains. It is worthy to note that studies of this kind are sparse in poly(ester–imide)s due to the insolubility of these polymers in nonpolar solvents.

This paper describes the synthesis of poly(ester–imide) chains from *N*-(4-carboxyphenyl)trimellitimide acid and diethylene glycol. The dipolar correlation coefficient of the chains is measured, and its value is interpreted using the rotational isomeric state (RIS) model. It is shown that by employing the Amber force field to calculate the energy associated with gauche states about OCH<sub>2</sub>–CH<sub>2</sub>O bonds of the spacer there is no need to invoke the *gauche effect*<sup>7,8</sup> to explain the difference observed between the experimental and the theoretical results obtained using other force fields. Attention is also paid to the influence of the distribution of units along the chains on the polarity of poly(ester–imide)s. Finally, the influence of the distribution of repeat units on the distribution of correlation angles between successive rods is investigated.

### Experimental Part

**Synthesis and Characterization of the Poly(ester–imide).** 1,5-Dihydroxy-3-oxapentane (diethylene glycol) (DEG) was vacuum distilled before use. The dimethyl ester of *N*-(4-carboxyphenyl)-4-carboxyphthalimide, **1**, was prepared by a method reported earlier.<sup>5</sup> The poly(ester–imide) was synthesized in a cylindrical glass vessel fitted with a mechanical stirrer and gas inlet and outlet tubes. DEG (11.13 g, 105 mmol), **1** (16.97 g, 50 mmol), and isopropyl titanate (0.0142 g, 0.05 mmol) were weighted into the vessel and heated by means of a metal bath, under a blanket of nitrogen. The mixture was heated to 200 °C, where the ester interchange reaction began, and then a gradual ramp was applied over 4 h up to a maximum temperature of 250 °C, with the final steps being carried out under a vacuum of approximately 1 mmHg. The viscous melt thus formed solidified upon cooling. It was dissolved in chloroform and precipitated with cold acetone. After intensive washing with acetone, the polymer PIEDEC was dried at 50 °C in a vacuum oven for 24 h. The yield was 96%.

The inherent viscosity, measured in chloroform, was 0.43 dL/g. The number-average molecular weight measured with

<sup>†</sup> Universidad de Alcalá.

<sup>‡</sup> CSIC.

**Table 1. Summary of Dielectric Results for the Poly(ester-imide) (PIEDEC) and the Model Compound NDDPT in Dioxane Solutions**

sample	<i>T</i> , °C	<i>dε/dw</i>	<i>2n<sub>1</sub>dn/dw</i>	$\langle \mu^2 \rangle$ , D <sup>2</sup>	$\langle \mu^2 \rangle/x$ , D <sup>2</sup>
model	30	2.78	0.34	11.63	
PIEDEC	30	4.55	0.49		12.70
	40	4.37	0.50		12.70
	50	4.22	0.52		12.73
	60	4.05	0.53		12.73

a Knauer vapor pressure osmometer was 13 600. The glass transition temperature, determined at a heating rate of 20 °C/min under nitrogen with a Perkin-Elmer DSC-7 calorimeter, was 101 °C.

The model compound, *N*-[4-[(decyloxy)carbonyl]phenyl]-4-[(decyloxy)carbonyl]phthalimide (NDDPT), was prepared in the same way as the polymer, by transesterification of **1** with 1-decanol catalyzed by isopropyl titanate at a temperature of 200 °C. The yield after recrystallization from *n*-heptane was 93%, and the melting point was 108 °C. Elem anal. Calcd: C, 73.10; H, 8.30; N, 2.36. Found: C, 72.83; H, 8.57; N, 2.29.

**Dielectric Measurements.** Values of the dielectric permittivity  $\epsilon$  of dioxane solutions of both the NDDPT model compound and the poly(ester-imide) were obtained, at 30 °C in the case of NDDPT and at 30, 40, 50, and 60 °C for the polymer, with a capacitance bridge (General Radio, type 1620 A) at 10 kHz, using a three-terminal cylindrical cell. The term  $d\epsilon/dw$ , proportional to the total polarization of the chains, was obtained at each temperature from the slope of the plots of the increments of the dielectric permittivity of the solutions with respect to that of the solvent,  $\Delta\epsilon = \epsilon - \epsilon_1$ , against the weight fraction of polymer  $w$ , in the limit  $w \rightarrow 0$ . Results for the increments of the index of refraction of the solutions,  $n$ , with respect to that of the solvent,  $n_1$ , were measured with a differential refractometer (Chromatix Inc.). From the slope of the plots  $\Delta n$  against  $w$ , the term  $dn/dw$ , proportional to the electronic polarization, was determined. The results for  $d\epsilon/dw$  and  $dn/dw$  are given in the third and fourth columns of Table 1.

Values of the mean-square dipole moment,  $\langle \mu^2 \rangle$ , were obtained for the poly(ester-imide) chains by means of the Guggenheim and Smith equation<sup>9,10</sup>

$$\langle \mu^2 \rangle = \frac{27k_B TM}{4\pi\rho N_A(\epsilon_1 + 2)^2} \left[ \frac{d\epsilon}{dw} - 2n_1 \frac{dn}{dw} \right]$$

where  $k_B$  and  $N_A$  are respectively the Boltzmann constant and Avogadro's number,  $T$  is the absolute temperature,  $M$  is the molecular weight of the solute, and  $\rho$  is the density of the solvent. Values of the mean-square dipole moment of NDDPT and the mean-square dipole moment per repeating unit of the polymer are given in the last two columns of Table 1. The uncertainty of these values was less than  $\pm 2.5\%$ . The temperature coefficient of the mean-square dipole moment, expressed in terms of  $d \ln \langle \mu^2 \rangle / dT$ , is lower than  $1 \times 10^{-4} \text{ K}^{-1}$ .

## Theoretical Analysis

**(A) Molecular Dynamics Simulations on the Model Compound.** The condensation of *N*-(4-carboxyphenyl)trimellitimide acid with diethylene glycol produces two types of repeating units whose structures are schematized in Figures 1 (unit A) and 2 (unit B). Chains containing exclusively units of type A or units of type B are identical (i.e., poly-A is indistinguishable from poly-B). However, different copolymers may be formed by varying the proportion of the two types of units (for instance, by employing fractions of A units,  $w_A$ , ranging from 0 to 1) and the sequence in which the two units appear along the chain.

We have employed the molecule of NDDPT, schematically represented in Figure 3, as the model compound

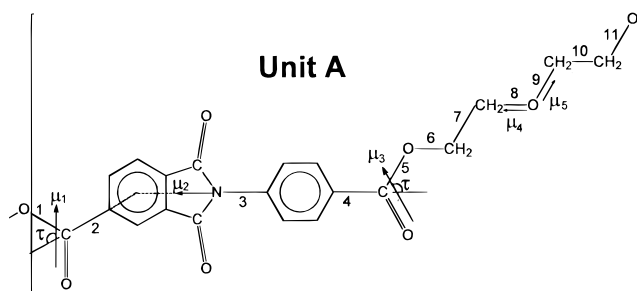


**Figure 1.** Schematic representation of the repeating unit of type A for PIEDEC shown in its planar *all-trans* structure. Contributions to the total dipole moment of the unit arising from ester ( $\mu_1$  and  $\mu_3$ ), imide ( $\mu_2$ ), and ether ( $\mu_4$  and  $\mu_5$ ) polar groups are represented by arrows pointing from negative to positive centers of charges.

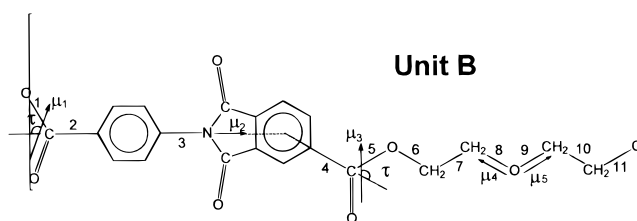


**Figure 2.** Schematic representation of the B kind of repeating unit for PIEDEC shown in its planar *all-trans* structure. See caption for Figure 1.

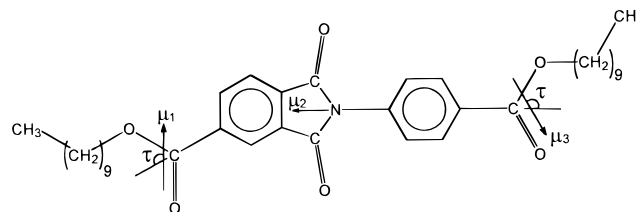


**Figure 3.** Structure of the NDDPT molecule that was used as a model compound for the acid residue on both A and B repeating units of PIEDEC in MD simulations. See caption for Figures 1 and 2.

for the acid residue of the repeating unit of the polymer. We have carried out molecular dynamics (MD) simulations of NDDPT in order to determine the conformational characteristics of bonds  $\text{CH}_2\text{-O}$ ,  $\text{O-C}^*$ ,  $\text{C}^*\text{-C}^{\text{ar}}$ , and  $\text{N-C}^{\text{ar}}$  that will be further used to formulate a statistical model for the polymer.

MD simulations of an isolated NDDPT molecule were performed with the DL POLY package<sup>11</sup> employing the Amber force field.<sup>12-14</sup> A time step  $\delta = 1 \text{ fs}$  (i.e.,  $10^{-15} \text{ s}$ ) was used for the integration cycle that was repeated  $10^7$  times to cover a total time span of 10 ns (i.e.,  $10^{-8} \text{ s}$ ) for the whole simulation. Conformations obtained after each 1000 steps were recorded, thus providing a total of  $10^4$  conformations for further analysis. The geometry of the molecule was first optimized with respect to all bond lengths, bond angles, and rotations by minimizing its conformational energy. This optimized geometry was then used as the starting point for the MD simulation, whose first assignment was to warm the molecule from 0 K to the working temperature with increments of 20 K and allowing a relaxation period of 500 fs at each intermediate temperature. Once the sample was stabilized at the desired temperature, the collection of data started. No scaling of the 1-4 interactions was performed. The Coulombic term of the potential energy was computed as the sum of pairwise interactions among partial charges, assigned to each

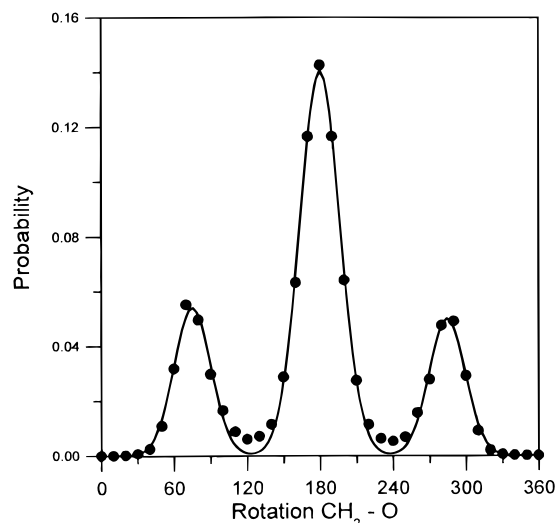


**Figure 4.** Probability distribution for  $\text{CH}_2\text{-O}$  bonds of the NDDPT molecule obtained from MD simulations performed at  $T = 500$  K and covering a time span of 10 ns. Filled circles represent the values actually obtained, while the solid line represents a least-squares fitting of those results and is drawn only to show the shape of the maxima.

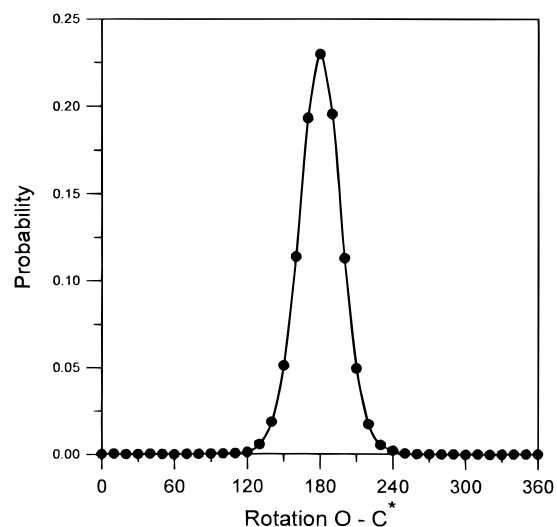


**Figure 5.** Same as Figure 4 for the ester  $\text{O-C}^*$  bonds.

atom of the molecule by means of the MOPAC package employing the AM1 procedure,<sup>15</sup> with a value of  $\epsilon = 4$  for the effective dielectric constant of the system.

Simulations on an isolated gas-phase molecule performed at  $T = 300$  K indicated that, even with a time span as large as 10 ns, the molecule did not visit all regions of conformational space in an equitable fashion. Thus, for instance, substantial differences were obtained among the values for the probabilities of the two equivalent planar orientations over bonds  $\text{C}^*-\text{C}^{\text{ar}}$ , i.e., the orientation shown in Figure 1 and that obtained after a  $180^\circ$  rotation over bond 4. For this reason, we have performed the calculation at a higher temperature, namely, at  $T = 500$  K, to facilitate passage over the rotational barriers and to ensure statistical sampling of the whole conformational space allowed to the molecule. The results obtained are summarized in Figures 4–7 which, represent the distribution of probabilities for the rotational states of the four kinds of bonds.

Figure 4 indicates that gauche states of  $\text{CH}_2\text{-O}$  bonds are located at  $\phi_g \approx \pm 75^\circ$ ; i.e., they are displaced by  $\Delta(\text{CH}_2\text{-O}) \approx 15^\circ$  from the perfectly staggered positions

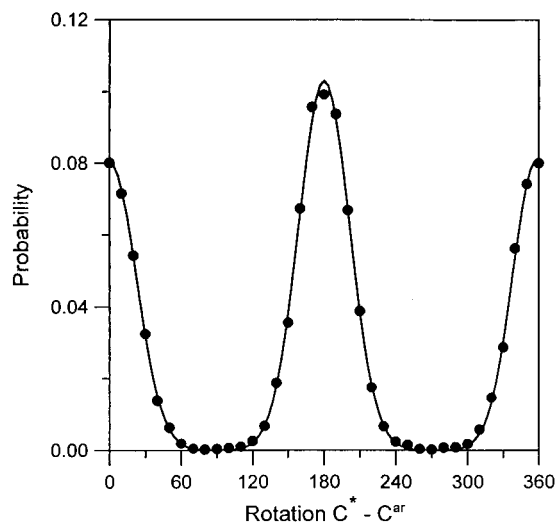


**Figure 6.** Same as Figure 4 for the  $\text{C}^*-\text{C}^{\text{ar}}$  bonds.

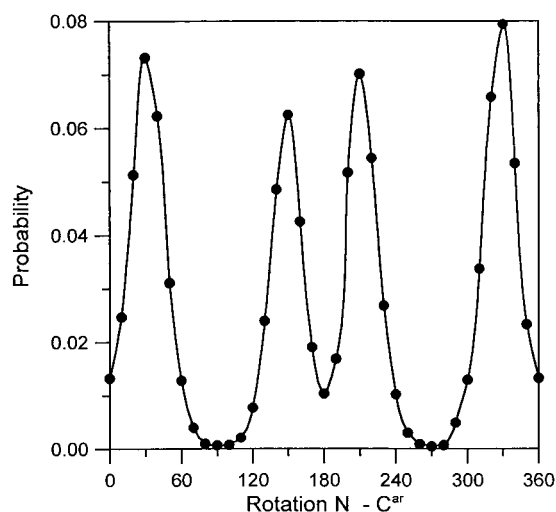


**Figure 7.** Same as Figure 4 for the  $\text{N-C}^{\text{ar}}$  bond.

and are strongly disfavored versus the alternative trans state, which is located at  $\phi \approx 180^\circ$ . Integration of the area under the peaks gives the probabilities for the three states as  $p_t = 0.60$ ;  $p_g \approx p_{g-} = 0.20$  at 500 K which represents an energy difference  $E_g \approx 1.1$  kcal/mol favoring the trans conformation. Values of both the displacement of gauche states and the conformational energy are in excellent agreement with the results obtained previously in an analysis of similar molecules.<sup>16</sup>

Figure 5 shows that, as might be expected, trans is the only orientation allowed for the ester  $\text{O-C}^*$  bond, which oscillates within the approximate limits  $\phi = 180 \pm 40^\circ$  but is incapable of surmounting its rotational barrier even at temperatures as high as 500 K. Bonds  $\text{C}^*-\text{C}^{\text{ar}}$ , which are represented in Figure 6, are located at the two planar orientations, i.e., trans with  $\phi_t = 180^\circ$  and cis with  $\phi_c = 0$ , approximately with the same probability. Finally, bond  $\text{N-C}^{\text{ar}}$ , whose probabilities are shown in Figure 7, has four allowed states which are displaced from the planar orientations by  $\Delta(\text{N-C}^{\text{ar}}) \approx 30^\circ$ , all four having roughly the same probability. The reason for this out-of-plane displacement is the interactions between  $\text{O}^*$  atoms of the imide and H atoms of the phenyl ring that are placed only ca. 1.9 Å apart in the planar conformations.

**Table 2. Set of Conformational Energies (in kcal/mol) Employed in the Present Work**

param	order	meaning	value	ref
$\sigma$	1	O-CH <sub>2</sub> in $g$	1.20	16
$\sigma_1$	1	OCH <sub>2</sub> -CH <sub>2</sub> O in $g$	-0.87	16
$\omega$	2	C*O-CH <sub>2</sub> -CH <sub>2</sub> in $g^{\mp}g^{\pm}$ (O...C*)	-0.13	16
$\gamma$	2	C*O-CH <sub>2</sub> -CH <sub>2</sub> in $g^{\pm}g^{\pm}$	-0.57	16
$\omega_1$	2	OCH <sub>2</sub> -CH <sub>2</sub> -O in $g^{\mp}g^{\pm}$ (CH <sub>2</sub> ...O)	0.36	21
$\omega_2$	2	CH <sub>2</sub> -O-CH <sub>2</sub> in $g^{\mp}g^{\pm}$ (CH <sub>2</sub> ...CH <sub>2</sub> )	$\infty$	21

The dipole moments of all the conformations adopted by the molecule along the MD trajectory were computed by determining the centers of gravity of the positive and negative charges assigned to each atom. Averaging of these results provides  $\langle\mu^2\rangle = 18.2 \text{ D}^2$ , which is noticeably larger than the experimental result of  $11.6 \text{ D}^2$  (see Table 1). However, it should be pointed out that the experimental result was obtained at  $30^\circ \text{C}$  while the calculations were performed at  $500 \text{ K}$  when substantial distortions of bond lengths and bond angles are produced that modify the charge distribution of the molecule.

An alternative procedure for obtaining the dipole moment of the NDDPT molecule is to sum the dipole contributions associated with its polar groups which in this case are two ester groups and one imide. The approximate directions of these dipoles are represented by arrows pointing from negative to positive centers of charges in Figure 3. Values  $\mu_1 = \mu_3 \approx 1.89 \text{ D}$  with a direction defined by the angle  $\tau \approx 121^\circ$  are customarily used for ester groups containing aromatic acid residues,<sup>7,17,18</sup> while  $\mu_2$  may be identified with the experimental dipole moment obtained for the *N*-methylphthalimide, which is approximately<sup>17</sup>  $2.24 \text{ D}$ . Averaging over the 16 conformations, each having identical probabilities, allowed to the polar central part of the NDDPT molecule (i.e., discarding the CH<sub>3</sub>-(CH<sub>2</sub>)<sub>9</sub>- segments at both ends) produces  $\langle\mu^2\rangle = 11.1 \text{ D}^2$ , which is in excellent agreement with the experimental result ( $11.6 \text{ D}^2$ ).

**B) Statistical Model for the Polymer.** The above results for the rotational states of the NDDPT molecule may be used to set up a conformational model for the two kinds of repeating units of the polymer. Thus, unit A contains 11 distinct rotatable bonds that are serially indexed from 1 to 11 in Figure 1. Bonds 6–11 (i.e., bonds of the O-CH<sub>2</sub> or CH<sub>2</sub>-CH<sub>2</sub> kind) have three allowed rotational isomers that will always be written in the order *trans* ( $\phi_t = 180^\circ$ ), *gauche* [ $\phi_g \approx -(60 + \Delta)^\circ$ ], and *negative gauche* [ $\phi_{g-} \approx (60 + \Delta)^\circ$ ]. Values  $\Delta(\text{O-CH}_2) = 15^\circ$ ,  $\Delta(\text{CH}_2\text{-CH}_2) = 0$  were used for the displacement of these two bonds from the staggered *gauche* positions. Only one isomer, with  $\phi_t = 180^\circ$ , is

allowed for O-C\* bonds such as 1 and 5. Bonds C\*-C<sup>ar</sup> such as 2 and 4 are allowed to have two orientations of the same energy that will be written in the order *trans* ( $\phi_t = 180^\circ$ ) and *cis* ( $\phi_c = 0$ ). Finally, bond 3 (N-C<sup>ar</sup>) has four energetically equivalent isomers that are separated by  $\Delta(\text{N-C}^{\text{ar}}) \approx 30^\circ$  from the planar orientations. Thus, the allowed positions for this bond are *trans*<sup>-</sup> ( $\phi_{t-} = 180 - \Delta_N$ ), *trans*<sup>+</sup> ( $\phi_{t+} = 180 + \Delta_N$ ), *cis*<sup>-</sup> ( $\phi_{c-} = -\Delta_N$ ), and *cis*<sup>+</sup> ( $\phi_{c+} = \Delta_N$ ). The statistical weight matrices representing all the allowed orientations for each pair of bonds within this unit may be written as follows:<sup>7,19,20</sup>

$$\begin{aligned} \mathbf{U}_1 &= [1] & \mathbf{U}_2 &= [1 \quad 1] & \mathbf{U}_3 &= \begin{bmatrix} 1 & 1 & 1 & 1 \\ 1 & 1 & 1 & 1 \end{bmatrix} \\ \mathbf{U}_4 &= \begin{bmatrix} 1 & 1 \\ 1 & 1 \\ 1 & 1 \end{bmatrix} & \mathbf{U}_5 &= \begin{bmatrix} 1 \\ 1 \end{bmatrix} & \mathbf{U}_6 &= [1 \quad \sigma \quad \sigma] \\ \mathbf{U}_7 &= \begin{bmatrix} 1 & \sigma_1 & \sigma_1 \\ 1 & \sigma_1\gamma & \sigma_1\omega \\ 1 & \sigma_1\omega & \sigma_1\gamma \end{bmatrix} & \mathbf{U}_8 &= \begin{bmatrix} 1 & \sigma & \sigma \\ 1 & \sigma & \sigma\omega_1 \\ 1 & \sigma\omega_1 & \sigma \end{bmatrix} \\ \mathbf{U}_9 &= \begin{bmatrix} 1 & \sigma & \sigma \\ 1 & \sigma & \sigma\omega_2 \\ 1 & \sigma\omega_2 & \sigma \end{bmatrix} & \mathbf{U}_{10} &= \begin{bmatrix} 1 & \sigma_1 & \sigma_1 \\ 1 & \sigma_1 & \sigma_1\omega_1 \\ 1 & \sigma_1\omega_1 & \sigma_1 \end{bmatrix} \\ & & \mathbf{U}_{11} &= \begin{bmatrix} 1 & \sigma & \sigma \\ 1 & \sigma\gamma & \sigma\omega \\ 1 & \sigma\omega & \sigma\gamma \end{bmatrix} \end{aligned}$$

where, as usual, matrix  $\mathbf{U}_i$  represents the pair of bonds  $i - 1$  and  $i$ , with the columns associated with the rotational isomers of bond  $i$  and the rows containing the isomers of bond  $i - 1$ . Table 2 summarizes the values of the conformational energies employed in the present work.

Serial multiplication of these matrices from  $\mathbf{U}_1$  to  $\mathbf{U}_{11}$  produces a  $1 \times 3\mathbf{U}_A$  matrix that represents the A unit and from which the partition function  $Z_A$  may be obtained as

$$Z_A = \mathbf{U}_A \begin{pmatrix} 1 \\ 1 \\ 1 \end{pmatrix} = \left[ \prod_{i=1}^{11} \mathbf{U}_i \right] \begin{pmatrix} 1 \\ 1 \\ 1 \end{pmatrix}$$

The  $\mathbf{M}$  matrices, required to compute the dipole moment of the whole molecule by vector addition of contributions assigned to every bond or group of bonds, may be formulated as<sup>7,19,20</sup>

**Table 3. Combination Rules Governing the Kind of U Matrix, Rotational States, Dipole Contributions, and Valence Angle That Should Be Merged Together To Build the Supermatrixes Associated with Each Bond of Both A and B Repeating Units of the PIEDEG Chain**

matrix	unit A				unit B			
	bond	states	$\mu$	$\theta$	bond	states	$\mu$	$\theta$
$\mathbf{U}_1$	O-C*	1	$\mu_1$	O-C*-C <sup>ar</sup>	O-C*	1	$\mu_1$	O-C*-C <sup>ar</sup>
$\mathbf{U}_2$	C*-C <sup>ar</sup>	2	0	$150^\circ$	C*-C <sup>ar</sup>	2	0	$180^\circ$
$\mathbf{U}_3$	N-C <sup>ar</sup>	4	$\mu_2$	$180^\circ$	C <sup>ar</sup> -N	4	$\mu_2$	$150^\circ$
$\mathbf{U}_4$	C <sup>ar</sup> -C*	2	0	C <sup>ar</sup> -C*-O	C <sup>ar</sup> -C*	2	0	C <sup>ar</sup> -C*-O
$\mathbf{U}_5$	C*-O	1	$\mu_3$	C*-O-CH <sub>2</sub>	C*-O	1	$\mu_3$	C*-O-CH <sub>2</sub>
$\mathbf{U}_6$	O-CH <sub>2</sub>	3	0	O-CH <sub>2</sub> -CH <sub>2</sub>	O-CH <sub>2</sub>	3	0	O-CH <sub>2</sub> -CH <sub>2</sub>
$\mathbf{U}_7$	CH <sub>2</sub> -CH <sub>2</sub>	3	0	CH <sub>2</sub> -CH <sub>2</sub> -O	CH <sub>2</sub> -CH <sub>2</sub>	3	0	CH <sub>2</sub> -CH <sub>2</sub> -O
$\mathbf{U}_8$	CH <sub>2</sub> -O	3	$\mu_4$	CH <sub>2</sub> -O-CH <sub>2</sub>	CH <sub>2</sub> -O	3	$\mu_4$	CH <sub>2</sub> -O-CH <sub>2</sub>
$\mathbf{U}_9$	O-CH <sub>2</sub>	3	$\mu_5$	O-CH <sub>2</sub> -CH <sub>2</sub>	O-CH <sub>2</sub>	3	$\mu_5$	O-CH <sub>2</sub> -CH <sub>2</sub>
$\mathbf{U}_{10}$	CH <sub>2</sub> -CH <sub>2</sub>	3	0	CH <sub>2</sub> -CH <sub>2</sub> -O	CH <sub>2</sub> -CH <sub>2</sub>	3	0	CH <sub>2</sub> -CH <sub>2</sub> -O
$\mathbf{U}_{11}$	CH <sub>2</sub> -O	3	0	CH <sub>2</sub> -O-C*	CH <sub>2</sub> -O	3	0	CH <sub>2</sub> -O-C*

$$\mathbf{M}_i = \begin{bmatrix} 1 & 2\mu^T \mathbf{T} & \mu^2 \\ \mathbf{0} & \mathbf{T} & \mu \\ 0 & 0 & 1 \end{bmatrix}_i$$

where  $\mu_i$  represents the dipole contribution associated with bond  $i$  and  $T(\phi_i, \theta_{i,i+1})$  indicates the matrix required to transform Cartesian coordinates from bond  $i+1$  to bond  $i$ ; it depends on the rotation  $\phi_i$  over bond  $i$  and the valence angle formed by bonds  $i$  and  $i+1$ .

Matrices  $\mathbf{U}$  and  $\mathbf{M}$  can now be combined, according to standard procedures,<sup>7,19,20</sup> to assemble supermatrices whose serial product provides the ensemble average  $\langle \mu^2 \rangle$ . Table 3 summarizes the combination rules, i.e., the kind of  $\mathbf{U}$  matrix, rotational states, dipole contributions, and valence angle that should be merged together.

The statistical weight matrices required for unit B are formally identical with those of unit A, and therefore serial multiplication of these matrices produces the same value of the partition function for both kinds of repeating units. However, as is indicated in Table 3, there are some differences in the magnitudes that appear in the  $\mathbf{M}_i$  matrices depending on whether they belong to an A or B unit. Consequently, the supermatrices and the result of  $\langle \mu^2 \rangle$  are different for the two kinds of units.

## Results and Discussion

All the calculations of the mean-square dipole moment  $\langle \mu^2 \rangle$  of the PIEDEG chain presented below were performed at  $T = 300$  K according to standard procedures of the matrix multiplication scheme.<sup>7,19,20</sup> Chains containing up to  $x = 100$  repeating units were generated with different relative numbers (i.e., fraction  $w_A$ ) and sequences of A and B units. The results shown for intermediate compositions (i.e.,  $0 < w_A < 1$ ) and random sequences are averages over the values obtained for 100 independently generated chains, each one of them containing the same fraction  $w_A$  and Bernoullian placement of both kinds of units. Typical values of the standard error of these averages amounted to ca.  $0.01 \text{ D}^2$ .

The following values were employed for the dipole contributions of the repeating units:<sup>7,17,18</sup> ester,  $\mu_1 \approx \mu_3 = 1.89 \text{ D}$  (experimental dipole of ethyl benzoate),  $\tau = 121^\circ$ ; imide,  $\mu_2 = 2.24 \text{ D}$  (from *N*-methylphthalimide); ether,  $\mu_4 = \mu_5 = 1.07 \text{ D}$  (i.e.,  $\mu = 1.23$  for the segment  $\text{CH}_2\text{--O--CH}_2$  in accordance with the experimental value for dimethyl ether).

Figure 8 summarizes the values of  $\langle \mu^2 \rangle$  obtained at  $300 \text{ K}$  as a function of the number of repeating units  $x$ , composition  $w_A$ , and sequence of A and B types of units. Typical differences among values of  $\langle \mu^2 \rangle$  computed with  $x = 50$  and  $x = 100$  are ca.  $0.02 \text{ D}^2$ , and for this reason, Figure 8 only shows the results obtained up to  $x = 50$ .

The dipole moment of a single B unit is substantially larger than that of an A unit. However, Figure 8 indicates that relatively short chains containing  $x > 20$  units produce the same result of  $\langle \mu^2 \rangle/x \approx 11.7 \text{ D}^2$  for both  $w_A = 0$  (only B units in the chain) and its equivalent composition  $w_A = 1$  that contains only A units. The polarity of the chain increases when both kinds of units are present, and again symmetrically equivalent compositions  $w_A = 0.25$  and  $0.75$  are different at low values of  $x$ , but they converge to the same limit  $\langle \mu^2 \rangle/x \approx 12.6 \text{ D}^2$  as the length of the chain increases. The maximum dipole moment among chains containing random sequences of B and A units is obtained at  $w_A = 0.5$  that

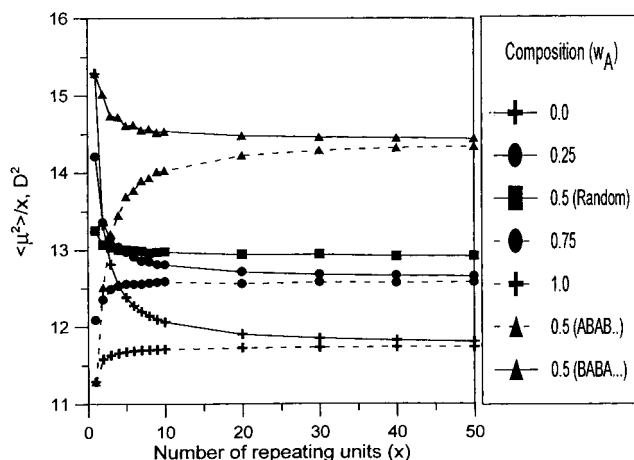


**Figure 8.** Mean-square dipole moment per repeating unit  $\langle \mu^2 \rangle/x$  computed at  $300 \text{ K}$  for the PIEDEG chain as function of the number of repeating units  $x$ . See text for details.

yields  $\langle \mu^2 \rangle/x \approx 12.9 \text{ D}^2$ , although this value is surpassed by chains with regular alternating sequences of A and B that tend toward  $\langle \mu^2 \rangle/x \approx 14.4 \text{ D}^2$  at high values of  $x$ , independent of whether they are started on A or B units.

It is interesting to notice that, assuming that the contributions to the total dipole moment were uncorrelated, a repeating unit of either A or B type would have  $\langle \mu^2 \rangle_{\text{uncorr}} = 2(1.89^2) + 2.24^2 + (2 \times 1.07 \cos 55^\circ)^2 = 13.7 \text{ D}^2$  which lies between the actual values computed for both kinds of units, suggesting that there are positive intra-unit correlations (i.e., reinforcement of contributions) in the structure of the B unit while the correlations are negative in the case of A units. Inter-unit correlations are important only for very low values of  $x$  since  $\langle \mu^2 \rangle/x$  remains constant for chains containing more than ca.  $x = 20$  units. These limiting results are larger than the uncorrelated values only in the case of alternating sequences of A and B units.

The sample synthesized for the present work was obtained by random condensation and, therefore, the experimental result  $\langle \mu^2 \rangle/x = 12.7 \text{ D}^2$  should be compared with the value obtained at  $w_A = 0.5$  with a random sequence of A and B units which amounts to  $12.9 \text{ D}^2$ . The good agreement between theory and experience suggests that the conformational model employed in the present work is appropriated for these kinds of molecules.

It is worth mentioning that the conformational energies  $E_\sigma$ ,  $E_{\sigma 1}$ ,  $E_\omega$ , and  $E_\gamma$  governing the conformations of the  $\text{O--CH}_2\text{--CH}_2$  sequence were obtained in the analysis of similar molecules<sup>16</sup> employing the Amber force field. Gauche states about  $\text{CH}_2\text{--CH}_2$  bonds which give rise to first-order interactions between two oxygen atoms have been reported to be disfavored with respect to the alternative trans states partially due to strong repulsive Coulombic contributions between the oxygen atoms. However, from the critical analysis of the dipole moment of dimethoxyethane and both the dipole moments and unperturbed dimensions of poly(ethylene oxide)<sup>8</sup> and poly(diethylene glycol terephthalate),<sup>22</sup> one finds that gauche states about  $\text{OCH}_2\text{--CH}_2\text{O}$  bonds have an energy of ca.  $0.5 \text{ kcal mol}^{-1}$  below that of the corresponding trans states. Similar discrepancies were observed for the energy of gauche states about  $\text{CH}_2\text{--O}$  bonds in poly(methylene oxide)<sup>8</sup> and other polyformals.<sup>23</sup> The disagreement observed between theory and experiment concerning the energy of gauche states in mol-

**Table 4. Variation of the Mean-Square Dipole Moment per Repeating Unit  $\langle \mu^2 \rangle/x$  (in D<sup>2</sup>) of the PIEDEG Molecule with the Dipole Contributions (in D) Employed in the Calculation<sup>a</sup>**

ester		imide $\mu_2$	ether $\mu_4 = \mu_5$	$\langle \mu^2 \rangle/x$
$\mu_1 = \mu_3$	$\tau$			
1.89	121	2.24	1.07	12.89
1.78	121	2.24	1.07	12.29
1.99	121	2.24	1.07	13.55
1.89	111	2.24	1.07	13.70
1.89	131	2.24	1.07	11.88
1.89	121	2.14	1.07	12.45
1.89	121	2.34	1.07	13.39
1.89	121	2.24	0.97	12.57
1.89	121	2.24	1.17	13.23

<sup>a</sup> Computations Were Performed at  $T = 300$  K with the Following Set of Conformational Energies (kcal/mol):  $E_G = 1.20$ ,  $E_{O1} = -0.87$ ,  $E_O = -0.13$ ,  $E_{O1} = 0.36$ ,  $E_{O2} = \infty$ ,  $E_Y = -0.57$ . All the results given in the table are averages over the values obtained for 100 independently generated chains each one containing 50 units of type A and 50 of type B with Brenoullian placement of both kinds of units. Standard error for the average amounted to ca. 0.01 D<sup>2</sup>.

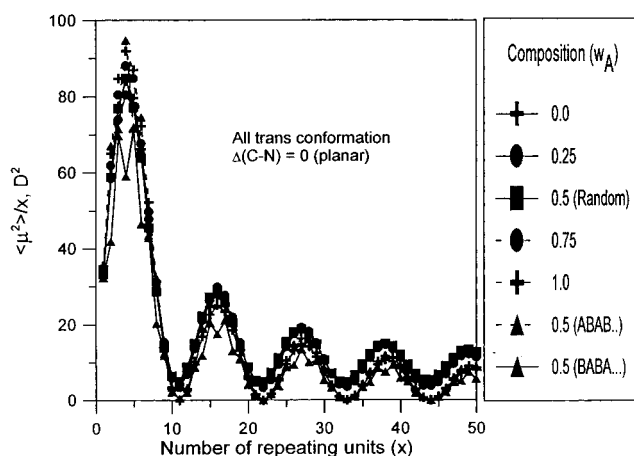
**Table 5. Variation of the Mean-Square Dipole Moment per Repeating Unit  $\langle \mu^2 \rangle/x$  (in D<sup>2</sup>) of the PIEDEG Molecule with Temperature (in K) and Conformational Energies (in kcal/mol) Employed in the Calculation<sup>a</sup>**

$E_G$	$E_{O1}$	$E_O$	$E_{O1}$	$E_{O2}$	$E_Y$	$T$	$\langle \mu^2 \rangle/x$
1.2	-0.87	-0.13	0.36	$\infty$	-0.57	300	12.89
1.0	-0.87	-0.13	0.36	$\infty$	-0.57	300	13.04
1.4	-0.87	-0.13	0.36	$\infty$	-0.57	300	12.77
1.2	-0.67	-0.13	0.36	$\infty$	-0.57	300	13.21
1.2	-1.07	-0.13	0.36	$\infty$	-0.57	300	12.68
1.2	-0.87	-0.33	0.36	$\infty$	-0.57	300	12.62
1.2	-0.87	0.07	0.36	$\infty$	-0.57	300	13.16
1.2	-0.87	-0.13	0.16	$\infty$	-0.57	300	12.80
1.2	-0.87	-0.13	0.56	$\infty$	-0.57	300	12.98
1.2	-0.87	-0.13	0.36	5	-0.57	300	12.90
1.2	-0.87	-0.13	0.36	$\infty$	-0.77	300	13.35
1.2	-0.87	-0.13	0.36	$\infty$	-0.37	300	12.51
1.2	-0.87	-0.13	0.36	$\infty$	-0.57	310	12.94
1.2	-0.87	-0.13	0.36	$\infty$	-0.57	290	12.88

<sup>a</sup> Computations were performed with the following set of dipole contributions: ester,  $\mu_1 \approx \mu_3 = 1.89$  D,  $\tau = 121^\circ$ ; imide,  $\mu_2 = 2.24$  D; ether,  $\mu_4 = \mu_5 = 1.07$  D. All the results were obtained as explained for Table 4.

ecules in which electronegative atoms intervene was reconciled by postulating a *gauche effect*. However, the use of the Amber force field seems to predict conformational energies about  $\text{OCH}_2\text{--CH}_2\text{O}$  bonds which are in reasonable agreement with the experimental results. Therefore, this force field shows its possible utility for the calculation of those conformational energies in which oxygen atoms intervene.

The variation of the dipole moment of the chain with the parameters used in the calculation is summarized in Tables 4 and 5. Table 4 shows the effect of the dipole contributions, the most important of which are those arising from the ester groups (in both module and orientation). Table 5 displays the effect produced by the energetic parameters on the polarity of the chains. It can be seen that variations of  $\pm 0.2$  kcal/mol in any of the conformational energies change the final result of  $\langle \mu^2 \rangle/x$  by less than 5%. The temperature coefficient, which can be estimated from the last two lines in Table 5, is negligible, as might be anticipated from the fact that different conformations allowed for the acid residue, that control the relative orientations of the most important contributions  $\mu_1$ ,  $\mu_2$ , and  $\mu_3$ , are symmetrically

**Figure 9.** Mean-square dipole moment per repeating unit  $\langle \mu^2 \rangle/x$  for the *all-trans* conformation of the PIEDEG chain as a function of the number of repeating units  $x$ . The whole acid residue was assumed to be planar, i.e.,  $\Delta(\text{N--C}^{\text{ar}}) = 0$ . See text for details.

equivalent, and therefore their statistical weights do not change with temperature.

At first sight, sequences of either A or B units in planar *all-trans* conformations seem to place the dipoles of the ester groups pointing in the same direction. The same effect occurs with the dipoles associated with the imide residue. This qualitative analysis would lead us to postulate that the *all-trans* conformation of poly(ester-imide) chains with the same types of units would have a high polarity. However, this assumption is not supported by the calculations. The dependence of  $\langle \mu^2 \rangle/x$  on the number of repeating units is plotted in Figure 9 for the unrealistic case in which the rotational angle about the  $\text{N--C}^{\text{ar}}$  bond is zero. The calculations show that for short chains the mean-square dipole moment per repeating unit increases, with  $x$  reaching a maximum for  $x = 5$ ; for  $x > 5$ ,  $\langle \mu^2 \rangle/x$  decreases sharply, coming close to zero for  $x = 10$ . For  $x > 10$  the shape of the variation of  $\langle \mu^2 \rangle/x$  with  $x$  resembles a damping wave. The cause of this behavior is that the macromolecule describes a planar spiral that places the dipoles in antiparallel directions whenever the molecule turns around. It is noteworthy that the dependence of  $\langle \mu^2 \rangle/x$  on  $x$  is independent of the distribution of A and B units along the poly(ester-imide) chains. If the calculations are repeated in the realistic case (rotational angle about  $\text{N--C}^{\text{ar}}$  bond =  $30^\circ$ ), one finds that the chain describes a non planar spiral. The dependence of the polarity of the chains on  $x$  is shown in Figure 10 where it can be seen that, in the cases in which the units are of the same type A (or B) or A and B are randomly distributed along the chains, the behavior is similar to that observed in Figure 9. However, if A and B are alternating, then  $\langle \mu^2 \rangle/x$  increases with  $x$  for values of  $x > 10$ .

One would expect, from the mesogenic character of the acid residue, that the poly(imide-ester)s exhibit thermotropic character. Earlier studies on the influence of the spacer on the correlation of two successive rods of thermotropic polyesters derived from *p,p'*-dibenzoic acid and polymethylene spacers  $(\text{CH}_2)_n$  showed that the correlation angle is strongly dependent on the even-odd character of the spacer.<sup>24-26</sup> Thus, if  $n$  is even, about 30% of the conformations form angles that lie in the range  $0\text{--}10^\circ$ , while for 70% of the conformers, this range lies between  $100$  and  $115^\circ$ . However, if  $n$  is odd, the value of the angle formed by two consecutive rods is ca.

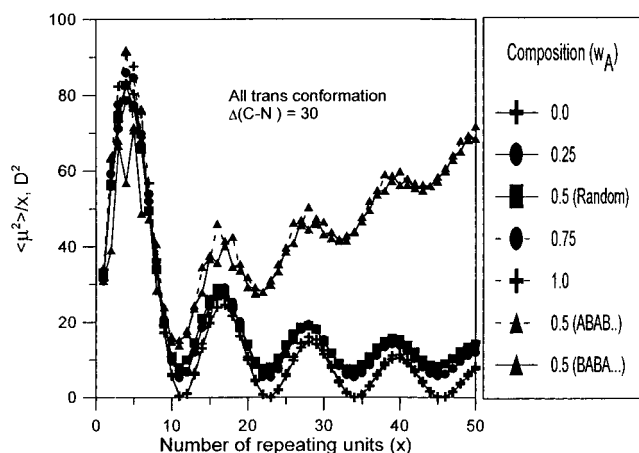


**Figure 10.** Same as Figure 9 with the more realistic value  $\Delta(N-C^{ar}) = 30^\circ$ .

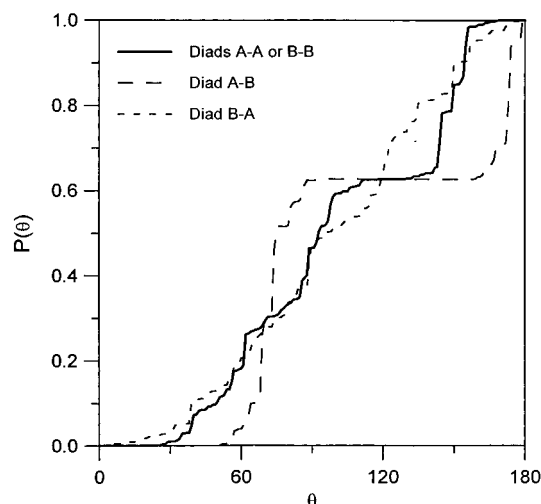


**Figure 11.** Integrated distribution curves for the angle  $\theta$  defined by the acid groups of two successive repeating units of the PIEDEG chain, taking as reference the vectors associated with the  $N-C^{ar}$  bonds.

$60^\circ$  for 80% of the conformations and ca.  $170^\circ$  for the remaining 20%.<sup>26</sup> Similar behavior was found when some of the  $CH_2$  groups in the spacers were replaced by ether groups.<sup>25</sup> The integral distribution of correlation angles between two consecutive units in the poly(imide-ester), taking the vectors associated with the  $N-C^{ar}$  bond of the mesogenic group as a reference, is shown in Figure 11. It can be seen that the distribution is bimodal and identical for A-A and B-B diads and, in the first step of the distribution, the curve for A-B diads is very similar to that of A-A (or B-B) diads. In these cases,  $P(\theta)$  is nearly continuously increasing from  $\theta \approx 30^\circ$  up to  $\theta \approx 120^\circ$ , with the value of  $P(120^\circ)$  being nearly 0.65. However, for diads B-A,  $P(\theta)$  undergoes a sharp increase at  $\theta \approx 60^\circ$  in a way similar to what

occurs for thermotropic polyesters derived from *p,p'*-dibenzoic acid separated by methylene spacers in which the number of methylene groups  $n$  is odd. By assuming that the integral correlations are similar for the melt and for isolated chains, the fact that  $P(\theta)$  is rather small for  $0 < 60^\circ < \theta$  suggests that the development of nematic order is not favored in poly(imide-ester) chains with diethylene glycol spacers. The development of smectic mesophases is not favored either because the correlation angles display a wide distribution of values of  $\theta$  lying in the range 30 and  $120^\circ$ .

**Acknowledgment.** This work was supported by DGICYT through Grants PB94-0364, PB95-0134-C02-01, and MAT95-0020.

## References and Notes

- (1) Kricheldorf, H. R.; Domschke, A.; Schwarz, G. *Macromolecules* **1991**, *24*, 1011.
- (2) de Abajo, J.; de la Campa, J. G.; Kricheldorf, H. R.; Schwarz, G. *Eur. Polym. J.* **1992**, *28*, 261.
- (3) Kricheldorf, H. R.; Hüner, R. *J. Polym. Sci., Part A: Polym. Chem.* **1992**, *30*, 337.
- (4) Kricheldorf, H. R.; Bruhn, C.; Rusanov, A.; Komarova, L. *J. Polym. Sci., Part A: Polym. Chem.* **1993**, *31*, 279.
- (5) Kricheldorf, H. R.; Schwarz, G.; de Abajo, J.; de la Campa, J. G. *Polymer* **1991**, *32*, 942.
- (6) Kricheldorf, H. R.; Schwarz, G.; de Abajo, J.; de la Campa, J. G. *Macromolecules* **1994**, *27*, 2540.
- (7) Riande, E.; Saiz, E. *Dipole Moments and Birefringence of Polymers*; Prentice-Hall: Englewood Cliffs, NJ, 1992.
- (8) Abe, A.; Mark, J. E. *J. Am. Chem. Soc.* **1976**, *98*, 6468.
- (9) Guggenheim, E. A. *Trans. Faraday Soc.* **1949**, *45*, 714; **1951**, *47*, 573.
- (10) Smith, J. W. *Trans. Faraday Soc.* **1950**, *46*, 394.
- (11) Forester, T. R.; Smith, W. DL POLY (Ver. 2.0), Daresbury Laboratory, Daresbury, Warrington, England.
- (12) Weiner, S. J.; Kollman, P. A.; Case, D. A.; Singh, U. C.; Ghio, C.; Alagona, G.; Profeta, S., Jr.; Weiner, P. *J. Am. Chem. Soc.* **1984**, *106*, 765.
- (13) Weiner, S. J.; Kollman, P. A.; Nguyen, D. T.; Case, D. A. *J. Comput. Chem.* **1986**, *7*, 230.
- (14) Homans, S. W. *Biochemistry* **1990**, *29*, 9110.
- (15) QCPE, Department of Chemistry, Indiana University, Bloomington, IN.
- (16) Saez-Torres, P.; Tarazona, M. P.; Saiz, E.; Riande, E.; Guzmán, J. *J. Chem. Soc., Perkin Trans. 2* **1998**, in press.
- (17) McClellan, A. L. *Tables of Experimental Dipole Moments*; Freeman: San Francisco, **1963**, Vol. I; Rahara Enterprises: El Cerrito, CA, 1974, Vol. II; 1989, Vol. III.
- (18) Saiz, E.; Hummel, J. P.; Flory, P. J.; Plavsic, M. *J. Phys. Chem.* **1981**, *85*, 3211.
- (19) Flory, P. J. *Statistical Mechanics of Chain Molecules*; Interscience: New York, 1969.
- (20) Flory, P. J. *Macromolecules* **1974**, *7*, 381.
- (21) Bravo, J.; Mendicuti, F.; Saiz, E.; Mattice, W. L. *Macromol. Chem., Phys.* **1996**, *197*, 1349.
- (22) San Román, J.; Guzmán, J.; Riande, E.; Santoro, J.; Rico, M. *Macromolecules* **1982**, *15*, 609.
- (23) Riande, E.; Mark, J. E. *Macromolecules* **1978**, *11*, 956.
- (24) Abe, A. *Macromolecules* **1984**, *17*, 2280.
- (25) Perez, E.; Riande, E.; Bello, A.; Benavente, R.; Pereña, J. M. *Macromolecules* **1992**, *25*, 605.
- (26) Bello, A.; Riande, E.; Pérez, E.; Marugán, M. M.; Pereña, J. M. *Macromolecules* **1993**, *26*, 1072.

MA9708196